ISSN 1541-308X, Physics of Wave Phenomena, 2021, Vol. 29, No. 4, pp. 352–362. © Allerton Press, Inc., 2021.

HYDRODYNAMICS OF ATMOSPHERE

Vertical Oscillations of Water Droplets in the Supporting Vapour–Air Flow

D. N. Gabyshev[a], *, A. A. Fedorets[a], and D. V. Shcherbakov[a]

[a] *X-BIO Institute, University of Tyumen, Tyumen, 625003 Russia*

**e-mail: d.n.gabyshev@utmn.ru*

Received July 6, 2021; revised August 19, 2021; accepted August 23, 2021

Abstract—A microscopic-size droplet levitates steadily in a vapor–air flow rising upward over a locally heated thin water layer. A Fourier analysis of the droplet position during a high-speed video recording revealed small-amplitude high-frequency droplet oscillations. This study focuses on overcoming the noise hindering extraction of oscillatory modes from spectra. The analysis revealed that some modes are associated with the horizontal droplet motion, while the others are due to the vertical motion. Possible physical reasons for the onset of this oscillatory motion are briefly discussed. Along with a single droplet, small clusters consisting of two or three droplets are considered.

Keywords: spectra, Fourier analysis, droplet oscillations, water aerosols, gas flow instability

DOI: 10.3103/S1541308X21040038

1. INTRODUCTION

The air medium hinders significantly the motion of rain droplets and clouds; the smaller the droplet size, the greater this hindrance is. It is most pronounced for fog or drizzle droplets from low stratiform and stratocumulus clouds, consisting of liquid droplets from 100 to 500 μm in diameter, with a terminal velocity up to few m/s. Precipitations of this type are most frequent over world oceans; they deteriorate visibility.

Each droplet perturbs the air medium through which it falls onto the earth ground. The pathlines of the medium flowing around the droplet according to the Coandă effect, form a potential well, in which the droplet is localized [1]. This well moves jointly with the droplet with a terminal velocity. A wakefield region formes behind the droplet, where random fluctuations and regular air microturbulences arise. As a result, the droplet is pushed by vortices, but it cannot deviate significantly from the vertical line because of the presence of potential well (in contrast to a Brownian particle). Researchers generally disregard the oscillatory component of motion and deal with only smoothed (dashed line in Fig. 1), well predictable droplet trajectories [2–4], despite the fact that the additional motion makes droplet to sweep a larger volume of space. Thus, it can be concluded, in particular, that droplet oscillations facilitate scavenging of solid aerosol dust particles from atmosphere [5]; they also affect the heat and mass transfer with the surrounding air (oscillating droplets are blown around more intensively). The latter factor facilitates the formation of the so-called virgas: broken tracks of droplets falling from nimbostratus clouds and evaporated before reaching the ground in hot and dry climates.

Due to the vibrational motion, microdroplets of any nature can float in air for a longer time. This is

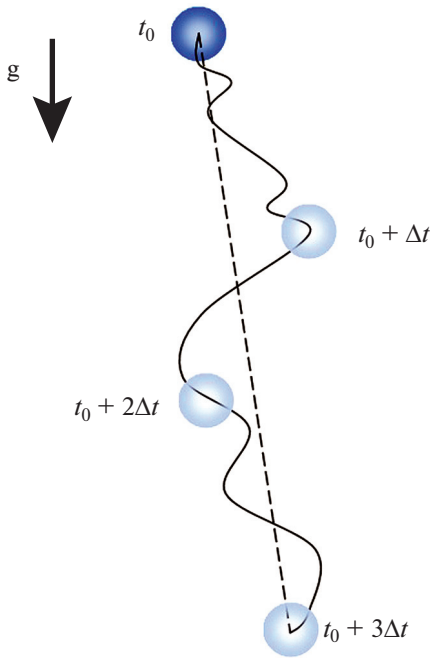

Fig. 1. (Color online) Schematic path of a falling drizzle droplet.

applicable in particular to droplets produced by coughing or sneezing [6–8]. Large raindrops falling on the soil disintegrate into smaller ones, which are carried away by air currents; these small droplets may contain bacteria from the soil helping them spread over a wider area [9]. Along with small droplets, soil particles are also splashed, causing a peculiar rain odor, known as petrichor [10]. Some agricultural diseases and pathogens can also be spread via airborne transmission [11]. There is no doubt that hovering of microdroplets in air because of their oscillations facilitates all the aforementioned phenomena.

Mechanical oscillations of liquid hydrometeors falling on the ground with a terminal velocity may occur in two directions: either perpendicular or parallel to the oncoming air flow direction. The oscillations in the perpendicular direction have recently been investigated using the droplet cluster technology [12]. A droplet cluster is an array of levitated water microdroplets, forming and self-organizing into a monolayer with an order close to hexagonal. Cluster droplets levitate above a locally heated flat water surface, because their weight is balanced by the ascending vapor–air flow. Their state is similar both to the state of droplets levitating in clouds and to the state of droplets falling down through the atmosphere, if we pass to the frame of reference in which a raindrop is on average at rest. As the cluster is localized at the center of a limited region of space, it is convenient for direct observations. In a series of papers published several years ago a first attempt was made to develop an analogy between a droplet cluster and the microstructure of clouds and fogs [13–15]. Further, the droplet cluster technology was used as a tool for studying the micrometeorological processes associated with single droplets or their clusters. The objects of study were the electric charge of droplets [16, 17], the electrically-driven coalescence [18] and condensational growth [19, 20] of droplets, as well as the influence of IR radiation [21] and electric field [22, 23] on their condensation. The inoculation of microorganisms into fog and cloud droplets was also investigated experimentally [24]. A decrease in the working temperature of droplets to room temperature gives grounds to expect generation of stable bioaerosols in future [25].

The study of planar horizontal oscillations (occurring perpendicularly to the flow of medium oncoming on a droplet from below) revealed a packet of frequencies in the range between 1.61 and 5.96 Hz, which are independent of both the mass of droplets and the sizes of a cluster formed by them [12]. The microturbulence vortices accompanying the droplet levitation in air (located between the droplet and water layer) were visualized later using tracer particles on the water surface [26].

The presence of high-frequency vertical oscillations of droplets (occurring along the oncoming airflow) was predicted theoretically in [27–29]. Here, we consider experimentally these vertical oscillations by an example of a levitated single droplet and small clusters consisting of two or three droplets. The first quantitative experimental observation of vertical oscillations of microdroplets at small Reynolds numbers ($\mathrm{Re} < 1$) was recently reported by the authors in cooperation with other researchers [30]. The emphasis of that publication was on the determination of the effective stiffness coefficient of the potential well in the vertical direction and its role in the stable levitation of droplet clusters. A problem of noise, which obscured the vertical oscillation frequencies and complicated the analysis, arose during the study. For this reason, a large amount of work aimed at minimizing noise and verifying the assignment of spectral peaks to vertical and horizontal oscillation directions was carried out. However, that part of the study remained beyond the frames of brief letter [30]. In this context, we would like to report here the data processing technique developed to solve the aforementioned problem. The issues concerning the influence of the recording frequency rate and the number and mass of droplets on the recorded spectral patterns are also considered.

2. EXPERIMENTAL

The details of the laboratory setup developed for observations were reported in [30]. Let us briefly recall them (Fig. 2). Microdroplets are formed and ordered into a cluster (*1*) above a thin (400 μm) horizontal water layer (*2*) containing a surfactant substance with a low concentration (sodium dodecyl sulfate, 0.5 g/L). The surfactant, as was shown in a special study [31], does not enter the composition of levitating droplets but suppresses the thermocapillary convection in the underlying water layer. The layer distributes over a Sitall substrate (*3*) of 400 μm thickness, glued on the metal base of a cuvette (*4*). The cuvette body contains a network of channels connected to a cryothermostat CC 805 (Huber, Germany), which serve to stabilize the water temperature at the cuvette periphery at a level of 10°C. Beam (*5*) of a semiconductor laser (MRL-III-660D-1W, CNI, China) performs a mediated local heating of water layer by heating the lower blackened surface of the substrate (*3*). The temperature distribution over the water surface is monitored by a thermal imager A655sc (FLIR, United States). The temperature at the heating spot center is monitored by a pyrometric sensor LT-CF2-CB3 (Micro-Epsilon, United States). If the concentration of condensation nuclei in the cuvette air is depleted to a value insufficient for cluster formation for some reasonable time (this may occur in a series of long-term experiments), an ultrasonic inhaler (A&D, Japan), filled with distilled water, can be used to generate clusters. Light penetrating through a hole (*6*) illuminates the cluster, whose image is directed by a mirror (*7*) to a micro-

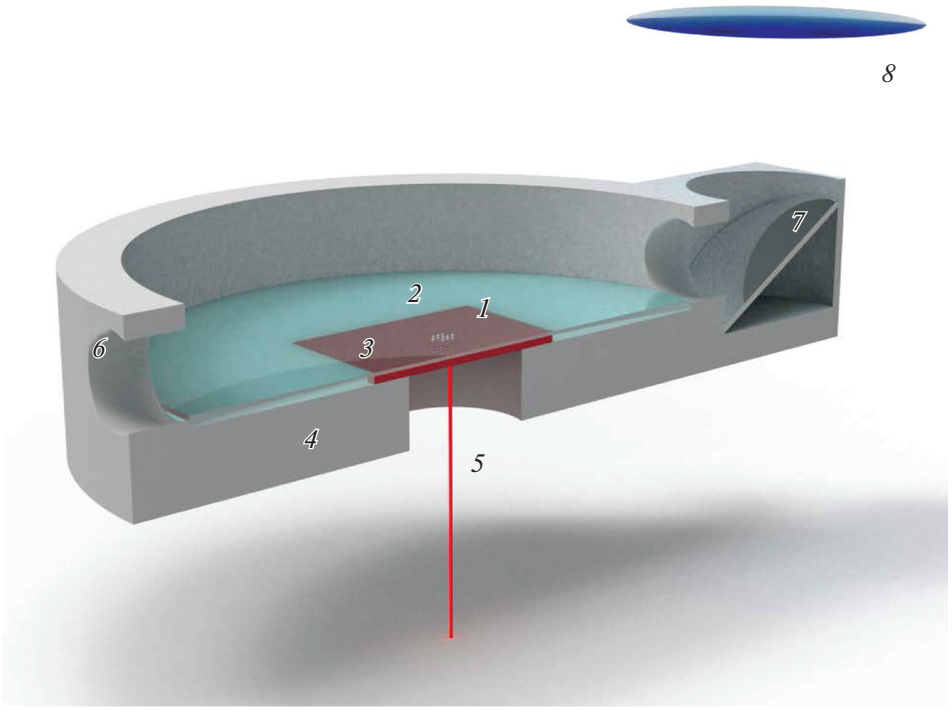

Fig. 2. (Color online) Schematic of the laboratory setup: (*1*) cluster, (*2*) thin water layer, (*3*) Sitall substrate, (*4*) cell base, (*5*) semiconductor laser beam, (*6*) hole, (*7*) mirror, and (*8*) microscope lens.

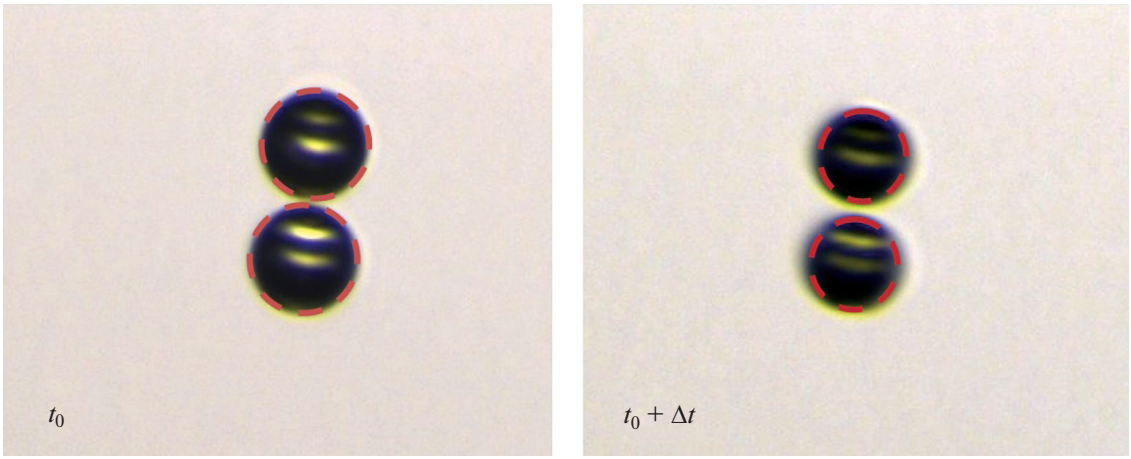

Fig. 3. (Color online) Photographs of a droplet (above) and its reflection (below) at two different instants (recording rate 150 s^{-1}, magnification 120X). Dashed lines show automatically recognized sizes.

scope lens (*8*). Thus, the droplet cluster is viewed aside.

One can limit the number of droplets using the following two-stage technique [19]. First, a cluster containing many droplets forms above the water surface. Then the power of laser beam (*5*) is sharply increased, so as to make the water surface temperature equal to $T = 62 \pm 1$°C throughout the central part of heated area. Droplets are ejected up by the enhanced vertical convective flow. Most of droplets are thrown beyond the observation field boundary. Then the laser power is reduced to the operating value. As a result, only one or two or several levitating droplets (objects of observation) remain, and the observation reference time is set. If the recording quality in some experiment is inadequate (the cluster image is strongly diffused), this experiment is repeated. Recording series are processed using a specially written computer software program,

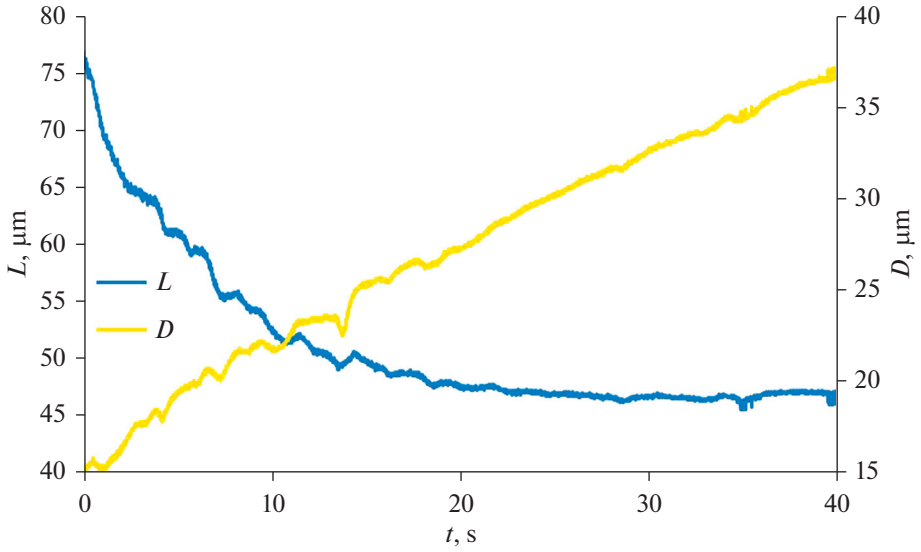

Fig. 4. (Color online) Typical plots of the recognized droplet diameter D and the distance L between the centers of droplet and its reflection.

which can recognize the droplet diameter (Fig. 3) and measure the distance between droplets and their reflections in water.

3. DATA PREPARATION

The droplets observed, being never at rest, oscillate incessantly rocking in the observation field. The intricate motion of a droplet is the result of superposition of the forces acting on it: the gravity force; the drag force from the side of vapor–air flow (close to the Stokes force [32, 33], but, nevertheless, somewhat deviating from it [34–36]); the buoyancy force acting on a body moving with acceleration [37]; periodic and almost periodic forces, related to the self-consistent vortices surrounding the droplet [26]; and uncontrolled random external forces, which are reduced to minimum.

The observer's line of sight makes a small angle ($\alpha = 3°$) with the water surface. This observation geometry allows one to observe simultaneously a droplet and its reflection in water through a microscope objective (see Fig. 3). The dataset extracted from a photograph contains the distance L between the centers of droplet and its reflection, as well as their diameters D. Initially all values are obtained in pixels. A single calibration on a scale ruler near the camera focus makes it possible to convert all values to micrometers.

When a droplet and its reflection are in the focus of microscope, their diameters can be determined fairly exactly. Swaying a droplet in the directions from and toward the observer by some distance Δx goes from the focus, and the image becomes diffuse. This diffusion affects the recognition of droplet diameter (see Fig. 3). Therefore, the value of recognized diameter oscillates in time with horizontal motion (Fig. 4), although in fact the true diameter should only gradually and monotonically increase because of the vapor condensation on the droplet.

Sets of values of the droplet diameter D and the distance L between the droplet and its reflection at each instant (see Fig. 4) were obtained for a single levitating droplet (at recording rates of 120, 150, and 180 fps), for a couple of droplets (at a rate of 180 fps), and for a triad of droplets (at a rate of 180 fps). It follows from Fig. 4 that the portions of plots in the second half of the observation range are more appropriate for analysis, because the droplet oscillations are less pronounced in this case (the center of mass of a falling droplet is intensively swinging, as box elder seeds do; this occurs until the droplet reaches its equilibrium position).

It is known that, along with the oscillatory motion, the droplet drifts in the field of view of video camera. The most pronounced is the linear drift, when the droplet center moves in space linearly with time. Since this drift is bad for Fourier analysis, it is expedient to eliminate it. Therefore, the following value must be subtracted from the initial dataset:

$$A_0 + A_1 t. \quad (1)$$

Here, A_0 and A_1 are the coefficients obtained by linear approximation of the initial set using the least-squares method. This procedure does not affect the recognition of desired frequencies but makes the pattern clearer. Even the quadratic term $A_2 t^2$ can be subtracted. A new dataset is obtained as a result of drift subtraction, which may be not completely free of drift because of the random character of the initial set. In this case

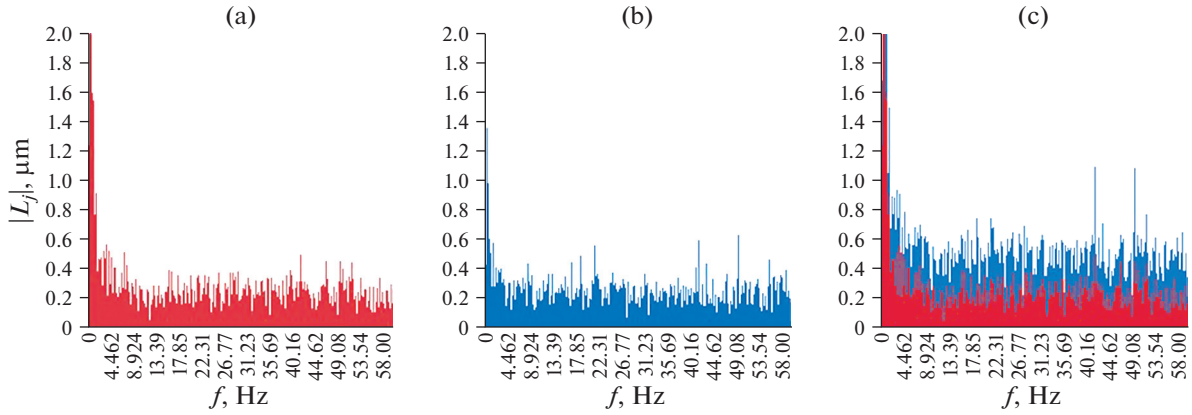

Fig. 5. (Color online) Illustration of the summation of spectra for the droplet–image distance: (a) some spectrum 1, (b) some spectrum 2, and (c) summary spectrum (1 + 2). One can observe amplified peaks.

the procedure can be repeated a desired number of times, until the data become free of drift.

The above-described procedure (detrending) is efficient on short time intervals. The droplet paths obtained in long-term observations are too intricate; in this case, one must subtract the trend obtained using, for example, the moving average or Savitzky–Golay method. Below we will analyze the data subjected to detrending using moving average over 60 neighboring points.

4. DATA ANALYSIS

The discrete fast Fourier transform [12]

$$L_j = \sum_{n=0}^{N-1} l_k \exp\left(-\frac{2\pi i}{N} kn\right), \quad k = 0,\ldots,N-1, \qquad (2)$$

where $N = 2^m$ is the number of observational frames and m is an integer, makes it possible to select the frequency response for a distance L (Fig. 5). When analyzing horizontal oscillations, it was concluded in [12] that the spectra cannot contain peaks caused by capillary oscillations [38], because their frequency exceeds the recording rate by several orders of magnitude. Oscillations of underlying water layer are also absent. Therefore, all observed mechanical oscillations of droplet are due to its interaction with the ascending vapor–air flow.

Since the amplitude of vertical oscillations is fairly small, the spectra of individual observations may barely have any pronounced peaks (see Figs. 5a, 5b). Obviously, strong peaks are obscured by noise. The quality can be improved by adding spectra (see Fig. 5). Here, two approaches can be applied. First, one can sum the spectra recorded for different clusters with the same number of droplets at the same recording rate. Second, the spectra from the same cluster obtained at different but closely spaced periods of time can be summed. Both these approaches are justified if there is no dependence on mass. If a cluster contains more than one droplet, the spectra for all droplets can also be summed. Finally, it is more interesting to pass to an averaged spectrum rather than only to sum spectra. We will apply these approaches below.

The following regularity can be seen in Fig. 4. The plots for the distance L and diameter D behave similarly: the positions of local valleys and convexities follow each other in the same way. The matter is that the photograph in Fig. 3 is a projection along the observer's line of sight. The vertical droplet displacement ΔL in this photograph is the sum of two values:

$$\Delta L = \Delta z \cos\alpha + \Delta x \sin\alpha, \qquad (3)$$

where α is the grazing observation angle. The first term in (3) is the projection of true vertical component Δz (change in the levitation height), a value of our interest, and the second term is the projection of horizontal motion from and toward an observer, Δx. Despite the fact that the angle α is small, the amplitude Δx is large: it reaches a value on the order of droplet diameter D. Therefore, a direct Fourier analysis of displacement (3) yields a mixed pattern, in which both vertical and horizontal droplet oscillations manifest themselves. The only way to separate oscillations in different directions is to take additionally into account the spectrum for recognized droplet diameter $D(t)$, in which the horizontal motion is encoded.

5. RESULTS

The influence of the droplet mass on spectra is illustrated in Fig. 6. To make this illustration, we chose four short successive intervals of observation (with a recording rate of 120 fps) of a single droplet with an average mass from 9 to 21 ng on each interval with a step of 3 ng. Each interval contains $2^9 = 512$ observational points. Since the average distance between the

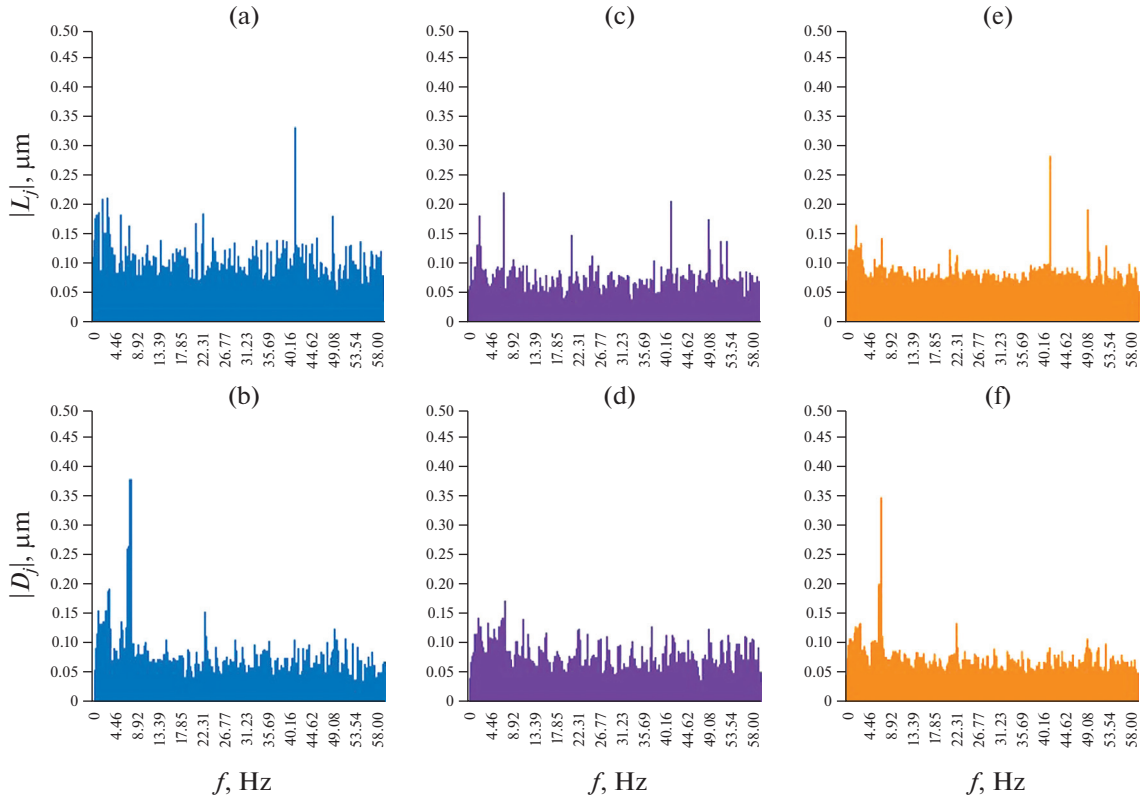

Fig. 6. (Color online) Influence of mass: spectra of the (a) distance L and (b) diameter D on the initial observation interval, spectra of the (c) distance L and (d) diameter D on the final observation interval, and the averaged spectra for the (e) distance L and (f) diameter D. The recording rate is 120 fps.

droplet and water surface decreases with an increase in mass, the droplet oscillations against the background of spectrum become less pronounced (see Figs. 6a, 6b, 6c, and 6d). For this reason, Figs. 6e and 6f show spectra averaged over four observation intervals.

The positions of significant peaks in spectra are independent of the droplet mass and observation instant (initial or final). Having compared the spectra for the levitation height L and the spectra for the diameter D (which contain a component of horizontal droplet motion from/toward an observer), one can conclude that 41.8 ± 0.2 and 49.5 ± 0.2 Hz are most likely vertical oscillation frequencies. The presence of a small peak at the same frequencies in the spectrum of D (see Figs. 6b, 6d) does not contradict this conclusion because the recognized droplet diameter is proportional to the value

$$\Delta D \sim -\Delta z \sin\alpha + \Delta x \cos\alpha. \quad (4)$$

Therefore, any significant vertical droplet displacement Δz may be manifested in the presence of the corresponding small peak in the diameter spectrum. Thus, expressions (3) and (4) are coupled, and any significant shift of droplet in one direction (x or z) should immediately manifest itself in both (L and D) spectra. With the best will, one cannot discriminate between vertical and horizontal oscillations applying a linear coordinate transformation to system (3) and (4), because expression (4) is linear only at a small droplet deviation, whereas the exact form of dependence (4) is yet unknown. The only conservative way to improve calculations is to choose the experimental portions of L and D plots that exhibit a relatively weak deviation from the trend line (1). Then one can expect that expression (4) is close to equality and that the true vertical displacement is $\Delta z = \Delta L \cos\alpha - \Delta D \sin\alpha$. Nevertheless, this way, being cumbersome, is beyond the scope of our study.

Thus, to attribute some frequency to vertical oscillations, its peak must be visualized only in the spectrum for height L and, ideally, be absent in the spectrum for diameter D (or, at least, the amplitude $|L_j|$ should exceed the amplitude $|D_j|$ at the same frequency). At frequencies of 41.8 and 49.5 Hz the amplitude $|L_j|$ exceeds $|D_j|$ by a factor of more than 3 and by a factor of 1.8, respectively (see Figs. 6e, 6f). In this context, the value of 41.8 Hz should be considered as more reliable. At the same time, it is doubtful that both frequencies are due to the video camera oscillation eigenfrequency, because the corresponding peaks have an irregular amplitude (the magnification is fixed).

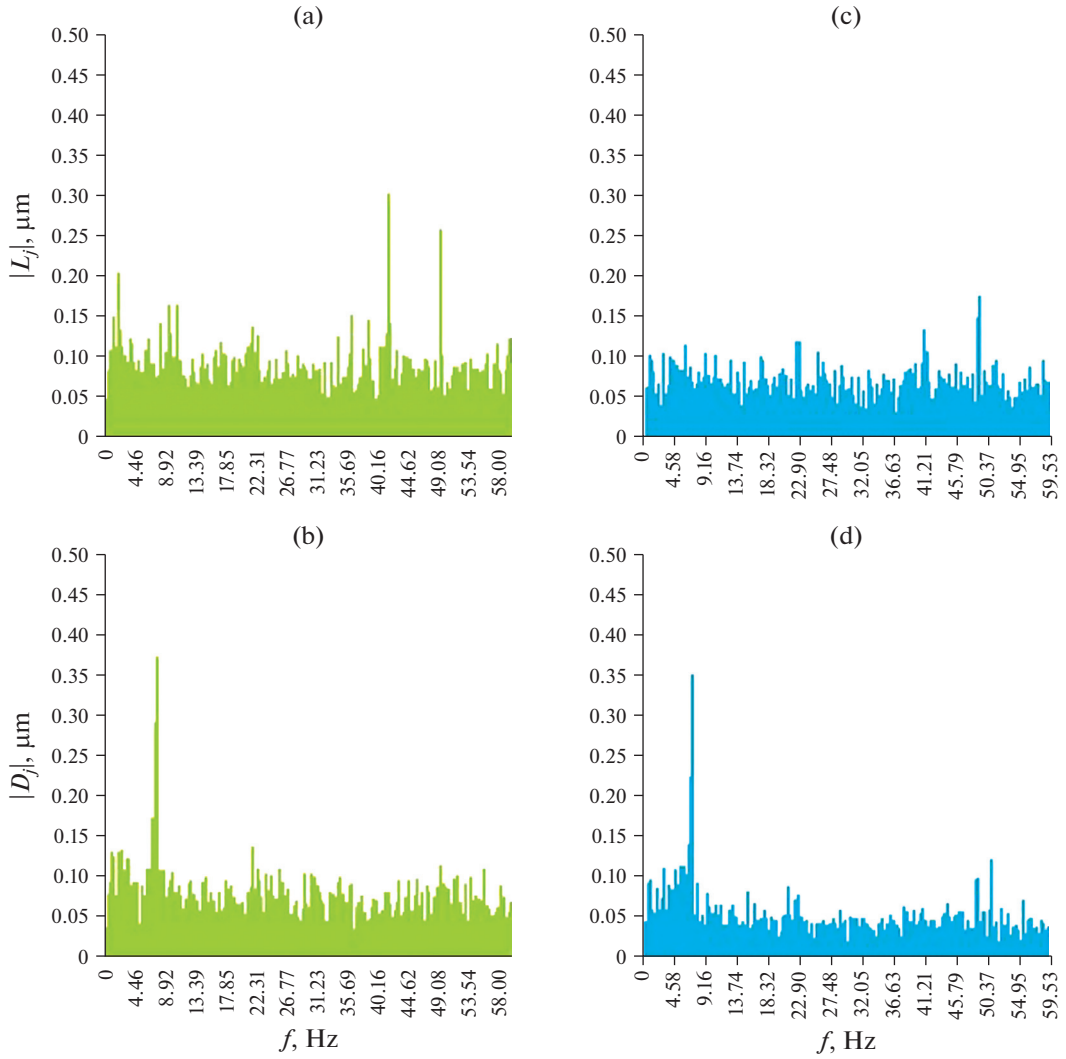

Fig. 7. (Color online) Influence of the recording rate: spectra averaged over observed (a, c) distances L and (b, d) diameters D for a single-droplet cluster at recording rates of (a, b) 150 and (c, d) 180 fps.

Let us briefly mention the hypothesis suggested by us, according to which the recording rate may affect the position of observed peaks. It was not justified when increasing the recording by 20%: from 150 to 180 fps (Fig. 7). No peaks with frequencies multiple of the recording rate were revealed. Therefore, there are no grounds to believe that the observed significant spectral peaks are due to instrumental errors.

All droplets in a cluster containing more than one droplet move synchronously due to the Huygens synchronization [39], because they interact through a gas interlayer. Any number of droplets (one, two, or three) in experiments leads to the same set of significant frequencies. The spectra for one-, two-, and three-droplet clusters at the maximum technically available frequency of 180 fps are compared in Fig. 8. The peaks at 41.8 and 49.5 Hz are present, as previously.

6. DISCUSSION

Since a spherical droplet is a poorly streamlined body, flow separation occurs on its lateral surface. There is a vortex stagnation zone behind the separation line. The separation line is not stable, and vortices from the stagnation zone periodically break loose, moving away along the flow. This is the mechanism of Kármán vortex street formation. The frequencies of vortex-induced oscillations in the transverse direction relatively to the flow are estimated via the Strouhal number as $f = \mathrm{St}v/D$. The Strouhal number St depends on the Reynolds number Re; at Re = 1 it can be equated approximately to 0.01 (extrapolating the well-known dependences to small Reynolds numbers [40, 41]). Then the oscillation frequency of a droplet 50 μm in diameter at an ascending flow velocity $v = 5$ cm/s [35] is about 10 Hz. This value coincides with the

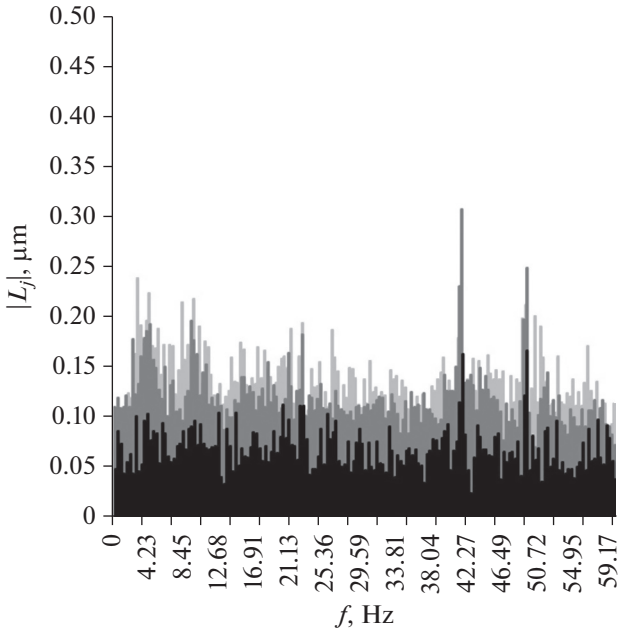

Fig. 8. Influence of the number of droplets: spectra of observed distances L for single droplets (black color), and two-droplet (gray) and three-droplet (bright gray) clusters. The recording frequency rate is 180 fps.

observed ones [12]. Speaking of the estimates for vertical oscillations, not everything is so clear.

Apparently, if a droplet does not shift for a fairly long time, it modifies locally (beneath and around it) the thermal field (the temperature under the lower droplet pole slightly exceeds that aside). The temperature field modification is a relatively slow process. Hence, being sharply shifted, a droplet resides for some time above a region with another temperature and, therefore, another vapor–air flow velocity. Obviously, the variations are very low but, at the same time, sufficient to change the vertical oscillation frequency. This logic explains (at least to some extent) the presence of two close maxima at frequencies of 41.8 ± 0.2 and 49.5 ± 0.2 Hz: one of them is related to the time intervals on which the droplet was at rest for a time sufficiently long to modify the temperature field, and the second is related to the intervals on which the droplet actively moved and, correspondingly, did not have enough time to modify the temperature field. This approach explains also why either the first or the second maximum is higher in different spectra: this pattern is determined by the ratio of the intervals of droplet mobility and rest, which changes fairly randomly from record to record. The gas flow relaxation time in the gap between the water layer and cluster is negligible. The relaxation time of a water droplet in the flow is much longer; specifically this parameter determines the time scale of the problem under consideration:

$$\tau = \rho D^2 / 36\mu,$$

where ρ is the water density in the droplet and μ is the dynamic viscosity of water vapor and air flowing around the droplet. At a droplet with a radius of 20 μm and a gas mixture viscosity of 15 μPa s we have $\tau = 5.9$ ms and the droplet eigenfrequency $f = 1/4\tau = 42$ Hz.

A droplet may be affected by gas flow field perturbations in a range of completely different frequencies. For a droplet suspended in viscous gas, the response to high-frequency oscillations of flow parameters is weak because of the significant droplet inertia. A decrease in the frequency of variations in gas flow parameters may lead to a situation where the period of external perturbations is comparable with the droplet dynamic relaxation time. In this case, one would expect a significant increase in the amplitude of droplet vertical oscillations. Under a constant periodic perturbation of the flow, the droplet oscillations are quasi-stationary and nondamping. To all appearances, specifically these oscillations were detected at frequencies of 41.8 ± 0.2 and 49.5 ± 0.2 Hz.

The presence of frequency peaks implies the existence of a potential well around the droplet. The ascending flow is laminar, but the presence of a droplet induces fairly regular turbulent micro-vortices, which form this well. The droplet is confined not only in the vertical direction but also in the horizontal plane. As was established in [12], the packet of eigenfrequencies of horizontal oscillations is mainly in the range of several hertz. Since the frequency of vertical oscillations is much higher, the potential well is more rigid in the vertical direction.

7. CONCLUSIONS

The presence of a microdroplet in the initially laminar ascending vapor–air flow gives rise to perturbations, which most likely become regular. The question about the nature of subsequent droplet motion remains not quite clear. Flow distortions may induce microturbulent vortices, which form a potential well around the droplet. However, the droplet oscillations can also be assigned to the Rayleigh–Taylor instability (similar to jerky outflow of liquid from a bottle with a narrow neck). Anyhow, the observation of these phenomena at small Reynolds numbers (Re < 1) is a unique result.

An attempt was made to detect vertical oscillation modes based on the original experimental technique. On the whole, the positions of peaks in the spectra were found to be reproducible. While carrying out the study, a problem of spectrum noisiness arose. To solve it, we performed averaging of spectra over different clusters with the same number of droplets, as well as averaging of spectra recorded for the same cluster on different but close periods of time. This approach is justified, because the position of the main peaks is independent on mass. It was found that the period when the levitation height changes weakly (a situation implemented in the second half of the observation period) is more appropriate for analysis. It was shown that a change in the recording rate does not lead to any shift of existing peaks or formation of spurious peaks. Finally, it became necessary to solve the problem related to the fact that the horizontal motion of droplet with respect to the observer manifests itself in the spectra for L according to expression (3). To understand which parts of the L spectrum are related to horizontal swaying, it was necessary to compare them with the spectra for recognized droplet diameter D, because the latter oscillates synchronously with the horizontal motion of droplet (the droplet leaves the focus, see Fig. 3).

We concluded that the spectral modes at frequencies of 41.8 ± 0.2 and 49.5 ± 0.2 Hz are due to vertical oscillations. Neither the recording rate nor the number of droplets affect the position of the corresponding peaks. The relatively large values (greatly exceeding the frequencies typical of horizontal oscillations [12]) show that the possible potential well confining the droplet is more rigid in the vertical direction. To validate the found values for vertical oscillation frequencies, it is necessary to perform more exact observations using an upgraded technique in order to minimize the above-described problems hindering the analysis.

ACKNOWLEDGMENTS

We thank Dr. L.A. Dombrovsky for the consultation.

FUNDING

The study was supported by the Council for Grants of the President of the Russian Federation (no. MK-819.2020.2) and the Ministry of Science and Higher Education of the Russian Federation (nos. 121040100270-2 and AAAA-A20-120051490005-9).

CONFLICT OF INTEREST

The authors declare that they have no conflicts of interest.

REFERENCES

1. L. G. Loitsyanskii, *Mechanics of Liquids and Gases* (Pergamon, Oxford, 1966).
2. L. R. Walton and J. N. Walker, "The trajectory of an evaporating water droplet falling in an airstream," *Trans. ASAE.* **13** (2), 0158–0161 (1970). https://doi.org/10.13031/2013.38560
3. J. A. Marchant, "Calculation of spray droplet trajectory in a moving airstream," *J. Agric. Eng. Res.* **22** (1), 93–96 (1977). https://doi.org/10.1016/0021-8634(77)90097-X
4. K. J. Finstad, E. P. Lozowski, and E. M. Gates, "A computational investigation of water droplet trajectories," *J. Atmos. Ocean. Tech.* **5** (1), 160–170 (1988). https://doi.org/10.1175/1520-0426(1988)005<0160:ACIOWD>2.0.CO;2
5. T. S. Pranesha and A. K. Kamra, "Scavenging of aerosol particles by large water drops: 1. Neutral case," *J. Geophys. Res.* **101** (D18), art. ID 23373 (1996). https://doi.org/10.1029/96JD01311
6. J. Atkinson, Y. Chartier, C. L. Pessoa-Silva, P. Jensen, Y. Li, and W.-H. Seto, *Natural Ventilation for Infection Control in Health-Care Settings* (World Health Organiz., Geneva, 2009). https://www.ncbi.nlm.nih.gov/books/NBK143284/
7. L. A. Dombrovsky, A. A. Fedorets, V. Yu. Levashov, A. P. Kryukov, E. Bormashenko, and M. Nosonovsky, "Modeling evaporation of water droplets as applied to survival of airborne viruses," *Atmosphere.* **11**, art. ID 965 (2020). https://doi.org/10.3390/atmos11090965
8. E. Bormashenko, A. A. Fedorets, L. A. Dombrovsky, and M. Nosonovsky, "Survival of virus particles in water droplets: Hydrophobic forces and Landauer's principle," *Entropy.* **23**, art. ID 181 (2021). https://doi.org/10.3390/e23020181
9. Y. S.Joung, Zh. Ge, and C. R. Buie, "Bioaerosol generation by raindrops on soil," *Nat. Commun.* **8**, art. ID 14668 (2017). https://doi.org/10.1038/ncomms14668
10. Y. S. Joung and C. R. Buie, "Aerosol generation by raindrop impact on soil," *Nat. Commun.* **6**, art. ID 6083 (2015). https://doi.org/10.1038/ncomms7083
11. S. Kim, H. Park, H. A. Gruszewski, D. G. Schmale, and S. Jung, "Vortex-induced dispersal of a plant

pathogen by raindrop impact," *Proc. Natl. Acad. Sci. U.S.A.* **116** (11), art. ID 4917 (2019). https://doi.org/10.1073/pnas.1820318116

12. A. A. Fedorets, N. E. Aktaev, D. N. Gabyshev, E. Bormashenko, L. A. Dombrovsky, and M. Nosonovsky, "Oscillatory motion of a droplet cluster," *J. Phys. Chem. C.* **123** (38), 23572–23576 (2019). https://doi.org/10.1021/acs.jpcc.9b08194
13. A. V. Shavlov, I. V. Sokolov, S. N. Romanyuk, and V. A. Dzhumandzhi, "Dropwise chains as the elements of water fog spatial structure," *Phys. Lett. A.* **377** (28–30), 1740–1744 (2013). https://doi.org/10.1016/j.physleta.2013.05.009
14. A. V. Shavlov, I. V. Sokolov, V. L. Hazan, and V. A. Dzhumandzhi, "Spatial structure of water fog," *Dokl. Earth Sci.* **461** (2), 422–426 (2015). https://doi.org/10.1134/S1028334X15040248
15. A. V. Shavlov, I. V. Sokolov, and V. A. Dzhumandzhi, "Viscosity and electric properties of water aerosols," *Dokl. Phys.* **61** (9), 429–434 (2016). https://doi.org/10.1134/S1028335816070132
16. A. V. Shavlov, V. A. Dzhumandzhi, and S. N. Romanyuk, "Electrical properties of water drops inside the dropwise cluster," *Phys. Lett. A.* **376** (1), 39–45 (2011). https://doi.org/10.1016/j.physleta.2011.10.032
17. A. A. Fedorets, L. A. Dombrovsky, E. Bormashenko, and M. Nosonovsky, "On relative contribution of electrostatic and aerodynamic effects to dynamics of a levitating droplet cluster," *Int. J. Heat Mass Transf.* **133**, 712–717 (2019). https://doi.org/10.1016/j.ijheatmasstransfer.2018.12.160
18. A. A. Fedorets, L. A. Dombrovsky, D. N. Gabyshev, E. Bormashenko, and M. Nosonovsky, "Effect of external electric field on dynamics of levitating water droplets," *Int. J. Therm. Sci.* **153**, art. ID 106375 (2020). https://doi.org/10.1016/j.ijthermalsci.2020.106375
19. A. A. Fedorets, M. Frenkel, E. Bormashenko, and M. Nosonovsky, "Small levitating ordered droplet clusters: Stability, symmetry, and Voronoi entropy," *J. Phys. Chem. Lett.* **8** (22), 5599–5602 (2017). https://doi.org/10.1021/acs.jpclett.7b02657
20. A. A. Fedorets, N. E. Aktaev, and L. A. Dombrovsky, "Suppression of the condensational growth of droplets of a levitating cluster using the modulation of the laser heating power," *Int. J. Heat Mass Transf.* **127A**, 660–664 (2018). https://doi.org/10.1016/j.ijheatmasstransfer.2018.07.055
21. L. A. Dombrovsky, A. A. Fedorets, V. Yu. Levashov, A. P. Kryukov, E. Bormashenko, and M. Nosonovsky, "Stable cluster of identical water droplets formed under the infrared irradiation: Experimental study and theoretical modeling," *Int. J. Heat Mass Transf.* **161**, art. ID 120255 (2020). https://doi.org/10.1016/j.ijheatmasstransfer.2020.120255
22. D. N. Gabyshev, A. A. Fedorets, N. E. Aktaev, O. Klemm, and S. N. Andreev, "Acceleration of the condensational growth of water droplets in an external electric field," *J. Aerosol Sci.* **135**, 103–112 (2019). https://doi.org/10.1016/j.jaerosci.2019.06.002
23. D. N. Gabyshev, A. A. Fedorets, and O. Klemm, "Condensational growth of water droplets in an external electric field at different temperatures," *Aerosol Sci. Technol.* **54**, 1556–1566 (2020). https://doi.org/10.1080/02786826.2020.1804522
24. A. A. Fedorets, E. Bormashenko, L. A. Dombrovsky, and M. Nosonovsky, "Droplet clusters: Nature-inspired biological reactors and aerosols," *Philos. Trans. R. Soc., A.* **377**, art. ID 20190121 (2019), https://doi.org/10.1098/rsta.2019.0121
25. A. A. Fedorets, L. A. Dombrovsky, and P. I. Ryumin, "Expanding the temperature range for generation of droplet clusters over the locally heated water surface," *Int. J. Heat Mass Transf.* **113**, 1054–1058 (2017). https://doi.org/10.1016/j.ijheatmasstransfer.2017.06.015
26. A. A. Fedorets, M. Frenkel, I. Legchenkova, D. V. Shcherbakov, L. A. Dombrovsky, M. Nosonovsky, and E. Bormashenko, "Self-arranged levitating droplet clusters: A reversible transition from hexagonal to chain structure," *Langmuir.* **35** (47), 15330–15334 (2019). https://doi.org/10.1021/acs.langmuir.9b03135
27. D. N. Gabyshev, "Damping oscillations of microdroplets of a droplet cluster in an external electric field," *Phys. Wave Phenom.* **26** (3), 221–233 (2018). https://doi.org/10.3103/S1541308X1803007X
28. S. N. Andreev and D. N. Gabyshev, "Oscillatory motion of microdroplets of a droplet cluster in a linearly nonuniform electric field," *Bull. Lebedev Phys. Inst.* **45** (9), 257–262 (2018). https://doi.org/10.3103/S1068335618090014
29. D. N. Gabyshev and A. A. Fedorets, "Electrically induced coalescence of droplet clusters in external electric fields," *J. Electrostat.* **112**, art. ID 103596 (2021). https://doi.org/10.1016/j.elstat.2021.103596
30. A. A. Fedorets, D. N. Gabyshev, D. Shcherbakov, E. Bormashenko, L. A. Dombrovsky, and M. Nosonovsky, "Vertical oscillations of droplets in small droplet clusters," *Colloids Surf., A.* **628**, art. ID 127271 (2021). https://doi.org/10.1016/j.colsurfa.2021.127271
31. A. A. Fedorets, D. Shcherbakov, L. A. Dombrovsky, E. Bormashenko, and M. Nosonovsky, "Impact of surfactants on the formation and properties of droplet clusters," *Langmuir.* **36**, 11154–11160 (2020). https://doi.org/10.1021/acs.langmuir.0c02241
32. A. A. Fedorets, I. V. Marchuk, and O. A. Kabov, "Role of vapor flow in the mechanism of levitation of a droplet-cluster dissipative structure," *Tech. Phys. Lett.* **37** (2), 116–118 (2011). https://doi.org/10.1134/S1063785011020064
33. A. A. Fedorets, M. Frenkel, E. Shulzinger, and L. A. Dombrovsky, "Self-assembled levitating clusters of water droplets: Pattern-formation and stability," *Sci. Rep.* **7** (1), art. ID 1888 (2017). https://doi.org/10.1038/s41598-017-02166-5
34. A. A. Fedorets, D. N. Gabyshev, I. V. Marchuk, and O. A. Kabov, "Droplets jump at the cluster coalescence

with the locally heated liquid layer," *Interfacial Phenom. Heat Transfer.* **8** (4), art. ID 337 (2020). https://doi.org/10.1615/InterfacPhenomHeatTransfer.2020037059

35. D. N. Gabyshev, D. N. Medvedev, and K. V. Misiiuk, "Dynamics of droplets ejected above an evaporating water surface," *Tekh. Fiz.* **91** (9), 1331–1338 (2021) [in Russian]. https://doi.org/10.21883/JTF.2021.09.51211.25-21
36. D. V. Zaitsev, D. P. Kirichenko, O. A. Kabov, and V. S. Ajaev, "Levitation conditions for condensing droplets over heated liquid surfaces," *Soft Matter.* **17**, 4623–4631 (2021). https://doi.org/10.1039/D0SM02185G
37. S. N. Manida, *Physics. Solution of Tasks of Elevated Complexity: Based on the Materials of the City Schoolchildren Olympiads: Tutorial* (St. Petersburg State Univ., St. Petersburg, 2004), pp. 10, 398 [in Russian].
38. G. Brenn, "Drop shape oscillations," in *Droplet Interactions and Spray Processes. Fluid Mechanics and Its Applications.* Ed. by G. Lamanna, S. Tonini, G. Cossali, and B. Weigand (Springer, Cham, 2020). Vol. 121.
39. A. R. Willms, P. M. Kitanov, and W. F. Langford, "Huygens' clocks revisited," *R. Soc. Open Sci.* **4** (9), art. ID 170777 (2017). https://doi.org/10.1098/rsos.170777
40. I. Kim and X. L. Wu, "Unified Strouhal–Reynolds number relationship for laminar vortex streets generated by different-shaped obstacles," *Phys. Rev. E.* **92**, art. ID 043011 (2015). https://doi.org/10.1103/PhysRevE.92.043011
41. H. Jiang and L. Cheng, "Strouhal–Reynolds number relationship for flow past a circular cylinder," *J. Fluid Mech.* **832**, 170–188 (2017). https://doi.org/10.1017/jfm.2017.685

Translated by Yu. Sin'kov